PNAS RESEARCH ARTICLE | DEVELOPMENTAL BIOLOGY

Perivascular cells support folliculogenesis in the developing ovary

Shu-Yun Li[a], Bidur Bhandary[a], Xiaowei Gu[a], and Tony DeFalco[a,b,1]

Edited by Thomas Spencer, University of Missouri, Columbia, MO; received July 30, 2022; accepted September 7, 2022

Supporting cells of the ovary, termed granulosa cells, are essential for ovarian differentiation and oogenesis by providing a nurturing environment for oocyte maintenance and maturation. Granulosa cells are specified in the fetal and perinatal ovary, and sufficient numbers of granulosa cells are critical for the establishment of follicles and the oocyte reserve. Identifying the cellular source from which granulosa cells and their progenitors are derived is an integral part of efforts to understand basic ovarian biology and the etiology of female infertility. In particular, the contribution of mesenchymal cells, especially perivascular cells, to ovarian development is poorly understood but is likely to be a source of new information regarding ovarian function. Here we have identified a cell population in the fetal ovary, which is a Nestin-expressing perivascular cell type. Using lineage tracing and ex vivo organ culture methods, we determined that perivascular cells are multipotent progenitors that contribute to granulosa, thecal, and pericyte cell lineages in the ovary. Maintenance of these progenitors is dependent on ovarian vasculature, likely reliant on endothelial–mesenchymal Notch signaling interactions. Depletion of Nestin^{+} progenitors resulted in a disruption of granulosa cell specification and in an increased number of germ cell cysts that fail to break down, leading to polyovular ovarian follicles. These findings highlight a cell population in the ovary and uncover a key role for vasculature in ovarian differentiation, which may lead to insights into the origins of female gonad dysgenesis and infertility.

perivascular cells | Nestin | ovary | blood vessels | ovarian follicle

Significance

A critical aspect of female fertility is the support of oocyte development within ovarian follicles by somatic supporting cells called granulosa cells. A sufficient number of granulosa cells is essential for establishing a reserve of ovarian follicles to ensure a long reproductive lifespan; therefore, an important question to address is how granulosa cells differentiate during folliculogenesis. Here we identify Nestin-expressing perivascular cells as multipotent progenitors that give rise to granulosa cells and other ovarian cell types. We show that endothelial cells maintain these progenitor cells in a perivascular niche via Notch signaling, and ablation of perivascular cells results in disrupted follicular development. These findings provide insights into the role of vasculature and its associated cells in promoting female fertility.

Testis and ovary organogenesis are unique processes in which two distinct organs can arise from a common gonadal primordium (1). Sex determination is initiated around embryonic day 11.5 (E11.5) in mice, at which time testes and ovaries undergo sex-specific molecular and morphogenetic changes (1, 2). In the absence of the *Sry* gene, the bipotential gonad undergoes ovarian development, ultimately leading to the formation of follicles consisting of a single oocyte surrounded by somatic granulosa cells. The fetal ovary is composed of ovarian surface epithelial cells, endothelial cells forming blood vessels, mesenchymal or stromal cells, granulosa (or pregranulosa) cells, and germ cells (3).

Granulosa cells play a critical role in supporting oocyte development by producing multiple hormones and growth factors in immature and mature follicles (4). The embryonic origins of granulosa cells are still not entirely clear. There are two classes of granulosa precursors that have been described in the fetal mouse ovary. The first class of granulosa cells, which express FOXL2 at early fetal stages, gives rise to medullary primordial follicles that are synchronously activated and become the first wave of active follicles after birth. The second class of follicle cells is composed of LGR5^{+} somatic cells, or coelomic epithelial cells at fetal stages, and gives rise to primordial follicles of the adult ovarian cortex that are gradually activated over the reproductive lifespan and, therefore, constitute the definitive oocyte reserve. Both medullary and cortical granulosa cells in the postnatal ovary are marked by the expression of FOXL2 (5–7).

Blood vessels are well known for delivering oxygen and nutrients to growing organs. However, recent studies have shown that blood vessels are a critical component of stem cell niches and play essential roles during organogenesis (8–10). Vascular development during gonadogenesis in mice first occurs around E11.5 in both sexes in a sexually dimorphic fashion (11), and blood vessels are critical for multiple aspects of testis morphogenesis (12, 13) and for testis differentiation (14).

In contrast to the fetal testis, little is known about the role of vasculature during ovary organogenesis (15). There are dense medullary networks of vessels, whose function is unclear, near clusters of germ cells known as ovigerous cords or germline cysts (16). VEGF (vascular endothelial growth factor) signaling is involved in early follicle activation, as well as angiogenesis, in the postnatal rat ovary (17); however, factors regulating ovary patterning, especially in the interstitial compartment during fetal and perinatal stages, remain largely unaddressed. In particular, ovarian perivascular cells are

Author affiliations: [a]Reproductive Sciences Center, Division of Developmental Biology, Cincinnati Children's Hospital Medical Center, Cincinnati, OH 45229; and [b]Department of Pediatrics, University of Cincinnati College of Medicine, Cincinnati, OH 45267

Author contributions: S.-Y.L. and T.D. designed research; S.-Y.L., B.B., X.G., and T.D. performed research; S.-Y.L. and T.D. analyzed data; and S.-Y.L. and T.D. wrote the paper.

The authors declare no competing interest.

This article is a PNAS Direct Submission.

[1]To whom correspondence may be addressed. Email: tony.defalco@cchmc.org.

This article contains supporting information online at http://www.pnas.org/lookup/suppl/doi:10.1073/pnas.2213026119/-/DCSupplemental.

Published October 4, 2022.

poorly understood, but in light of a single-cell RNA-sequencing study (scRNA-seq) indicating that perivascular cells are a major constituent of human ovaries (18), it is likely that perivascular cells play unappreciated roles in ovarian development. As of yet, ovarian cell types that arise from perivascular cells have not been rigorously defined.

Notch signaling integrates niche signals to direct cell differentiation during organ morphogenesis, including testis and ovary organogenesis (14, 19–21). Activation of the Notch pathway in the ovary has been implicated in vascular development, somatic–germline communication during folliculogenesis, preovulatory granulosa cell steroidogenesis, and regulation of meiosis in oocytes (19, 21, 22). However, the cellular players involved in fetal and postnatal ovarian Notch signaling are poorly understood and, in particular, links between Notch signaling, vascular–mesenchymal interactions, and perivascular cells remain major outstanding questions in the field.

In this study, we have used genetic lineage tracing assays and ex vivo organ culture approaches to address the origins and roles of vasculature and perivascular cells in the mouse ovary. We show that ovarian vasculature is critical for maintaining a multipotent progenitor niche that gives rise to several cell types, including granulosa cells, theca cells, and pericytes. These perivascular progenitors express Nestin, a marker for neural stem cells and stem-like progenitor cells in various organs (14, 23–25). Inhibition of vasculature disrupted the maintenance of Nestin$^+$ progenitor cells and induced their differentiation into granulosa cells during a specific developmental window. Cell-type–specific genetic deletion analyses revealed that maintenance of these progenitors in vivo was dependent on vascular-dependent Notch signaling within perivascular cells in the perinatal ovary. Finally, we specifically ablated postnatal Nestin$^+$ cells and found that granulosa cell specification was disrupted, leading to defective folliculogenesis and an increased occurrence of polyovular follicles. Our results uncover an instructive role for ovarian vasculature in the progenitor niche for granulosa cells, which is essential for establishing follicles, the structural and functional units of the ovary. These findings provide insights into basic mechanisms underlying organogenesis and highlight how vasculature and perivascular cells are vital components of ovarian development.

Results

Undifferentiated Perivascular Cells Express Nestin in the Fetal Ovary. Given that testes and ovaries arise from a common primordium, i.e., the bipotential gonad, we investigated whether Nestin$^+$ progenitors exist in the fetal ovary. Immunofluorescence analyses of E12.5 fetal ovaries revealed that Nestin protein was specifically enriched adjacent to ICAM2$^+$ blood vessels (Fig. 1*A*). To address whether Nestin-expressing cells were endothelial or perivascular cells, *Nestin*-CreER;*Rosa*-Tomato mice were used to permanently label Nestin$^+$ cells and their progeny in the ovary. To induce CreER activity, we injected 4-hydroxytamoxifen (4-OHT) intraperitoneally into pregnant females at E12.5, upon the first appearance of differentiated pregranulosa cells. Analyses of E13.5 and E18.5 *Nestin*-CreER;*Rosa*-Tomato fetal ovaries revealed that Tomato$^+$ cells expressed the pericyte marker CSPG4 (also known as NG2) (Fig. 1 *B* and *C*) and did not express the endothelial nuclear marker ERG (Fig. 1 *D* and *E*), demonstrating that Nestin$^+$ cells are perivascular stromal cells.

To further confirm that Nestin$^+$ cells are perivascular cells, gonadal cells were dissociated from E13.5 *Nestin*-CreER;*Rosa*-Tomato fetal ovaries after 4-OHT exposure at E12.5 and subjected to flow cytometric analysis. Our analyses showed that almost all Tomato$^+$ cells expressed CSPG4, but very few Tomato$^+$ cells expressed the endothelial marker PECAM1 (*SI Appendix*, Fig. S1 *A–C*). These data demonstrate definitively that Nestin-derived cells are perivascular, pericyte-like cells in fetal ovaries and are not endothelial cells.

We next assessed proliferation and cell cycle status of Nestin-derived cells in the fetal ovary. Flow cytometric analyses revealed no significant difference in the percentage of Tomato$^+$ cells within E13.5 versus E18.5 *Nestin*-CreER;*Rosa*-Tomato ovaries exposed to 4-OHT at E12.5 (Fig. 1*F*), potentially suggesting a low rate of proliferation. We used 5-ethynyl-2′-deoxyuridine (EdU) incorporation assays to examine the proliferative activity of Tomato$^+$ cells. EdU$^+$ cells were abundant in E13.5 and E18.5 *Nestin*-CreER;*Rosa*-Tomato fetal ovaries, but EdU was rarely detected in Tomato$^+$ cells (Fig. 1*G*). EdU assays revealed no significant difference in the percentage of EdU$^+$ Tomato-expressing cells within E13.5 versus E18.5 ovaries (Fig. 1*G*), suggesting Tomato$^+$ cells initially labeled at E12.5 did not significantly proliferate relative to other cell types, such as the surface coelomic epithelium, which displayed a much higher percentage of EdU$^+$ cells (*SI Appendix*, Fig. S1*D*). Consistent with a low rate of proliferation, Tomato$^+$ cells were predominantly MIK67$^-$ in late fetal ovaries (*SI Appendix*, Fig. S1 *E–G*).

Despite a low rate of proliferation in Tomato$^+$ cells, *Nestin* expression progressively increased in the ovary during fetal and postnatal stages, peaking at postnatal days 1 to 3 (P1-3) (*SI Appendix*, Fig. S1*H*). *Cdh5* (also called *VE-Cadherin*), an endothelial-specific gene, followed a similar pattern of expression during fetal stages and was maintained after birth (*SI Appendix*, Fig. S1*I*), consistent with a link between vascularization and *Nestin* expression. These data suggest that perivascular Nestin$^+$ cells initially labeled at E12.5 did not self-renew or expand to a large extent, but instead new Nestin$^+$ cells were continuously induced or recruited throughout development.

Perivascular Nestin$^+$ Cells Are Derived from Gonadal NR5A1$^+$ Somatic Cells. We next sought to determine the origin of Nestin$^+$ cells, which in the fetal ovary could potentially be the surface epithelium, gonadal mesenchyme, or mesonephros (26). To test whether Nestin$^+$ cells were derived from ovarian surface epithelium, MitoTracker dye was used to label the surface cells of E11.5 and E12.5 fetal ovaries, followed by ex vivo organ culture. At initial timepoints, the dye was clearly confined to the surface epithelium of E11.5 and E12.5 gonads (*SI Appendix*, Fig. S2 *A* and *C*). Nestin$^+$ cells within the interior of the gonad after culture for 48 h were not labeled with MitoTracker (*SI Appendix*, Fig. S2 *B* and *D*).

To further address the possibility that Nestin$^+$ cells arise from surface epithelial cells, we examined Nestin protein expression in E13.5 *Lgr5*-CreER;*Rosa*-Tomato ovaries exposed to 4-OHT at E12.5 to permanently label *Lgr5*-derived cells that originate from surface epithelium. Tomato$^+$ cells did not express Nestin (*SI Appendix*, Fig. S2*E*), suggesting that gonadal mesenchymal Nestin$^+$ cells adjacent to vasculature did not arise from the coelomic surface epithelium of the fetal ovary. Furthermore, we assessed LGR5 protein expression in E13.5 *Nestin*-CreER;*Rosa*-Tomato fetal ovaries exposed to 4-OHT at E12.5 and observed that Tomato$^+$ cells were LGR5$^-$ (*SI Appendix*, Fig. S2*F*).

To determine whether Nestin$^+$ cells are derived from the gonad or mesonephros, we examined the expression of NR5A1 (also called SF1 or Ad4BP), which is restricted to early gonadal

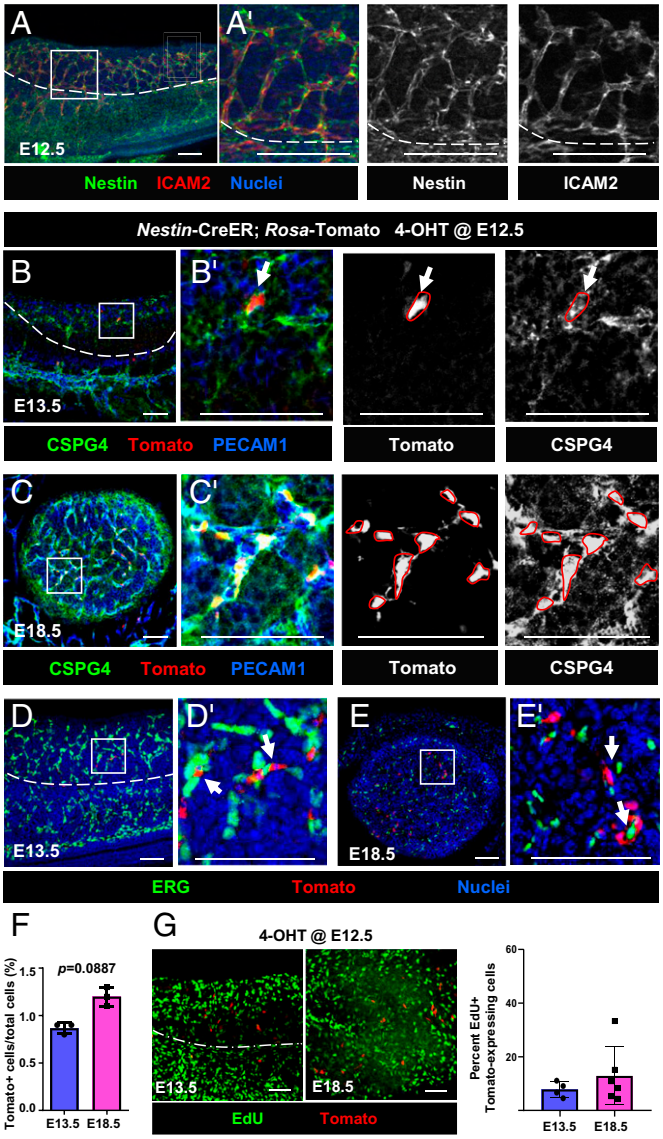

Fig. 1. Fetal ovarian Nestin$^+$ cells are perivascular, pericyte-like cells. (*A*) E12.5 wild-type CD-1 fetal ovary. (*B–E*) E13.5 (*B* and *D*) and E18.5 (*C* and *E*) *Nestin*-CreER;*Rosa*-Tomato fetal ovaries exposed to 4-OHT at E12.5. Tomato is expressed in CSPG4$^+$ (NG2$^+$) perivascular cells (arrows) but not in ERG$^+$ endothelial cells. (*F* and *G*) Flow cytometric analyses (*F*; $n = 3$ for E13.5 and E18.5) and EdU incorporation assays (*G*; $n = 4$ for E13.5 and $n = 6$ for E18.5) of E13.5 and E18.5 *Nestin*-CreER;*Rosa*-Tomato fetal ovaries exposed to 4-OHT at E12.5. Dashed lines indicate gonad–mesonephros border; *A′–E′* are higher-magnification images of the boxed regions in *A–E*. (Scale bars: 50 μm.)

somatic cells, but is not expressed in the mesonephros, and gives rise to pregranulosa cells and potential steroidogenic precursor cells (27, 28). In E13.5 *Nestin*-CreER;*Rosa*-Tomato ovaries exposed to 4-OHT at E12.5, most Tomato-labeled cells overlapped with NR5A1 (*SI Appendix*, Fig. S3*A*). In contrast, most Tomato-labeled cells did not colocalize with WT1, which is expressed in both gonad and mesonephric mesenchyme and contributes to the theca cell lineage (29) (*SI Appendix*, Fig. S3*B*). To investigate further whether Nestin$^+$ cells belong to the NR5A1$^+$ cell lineage, we examined Nestin expression in E13.5 and P2 *Nr5a1*-Cre;*Rosa*-Tomato fetal ovaries; we observed that perivascular Nestin$^+$ cells expressed Tomato (*SI Appendix*, Fig. S3 *C* and *D*). Our data suggest that ovarian perivascular Nestin$^+$ cells arise from gonadal NR5A1$^+$ somatic cells, indicating that these early cells potentially give rise to pregranulosa cells.

Nestin$^+$ Cells in the Developing Ovary Give Rise to Adult Granulosa Cells, Theca Cells, and Steroidogenic Interstitial Cells. To determine the adult ovarian cell types that arise from early fetal perivascular Nestin$^+$ cells, we examined P60 *Nestin*-CreER; *Rosa*-Tomato ovaries that were exposed to 4-OHT at E12.5. By P60, Tomato-labeled cells did not express Nestin protein, indicating that Nestin-derived cells had differentiated and subsequently lost expression of Nestin (Fig. 2*A*). To address the hypothesis that Nestin$^+$ cells are granulosa cell precursors, we examined the granulosa cell marker FOXL2. A subset of Tomato-labeled cells expressed FOXL2 (Fig. 2*B*), indicating that Nestin$^+$ cells are progenitors of granulosa cells. However, the number of Tomato$^+$ cells was likely underestimated at P60, because the number of 4-OHT–induced Tomato$^+$ cells at 12.5 was limited (likely due to CreER inefficiency) and new Nestin$^+$ progenitors likely emerged following the continued formation of blood vessels during development. To further examine this hypothesis, we administered 4-OHT at E15.5, E18.5, P2, and P4 in *Nestin*-CreER;*Rosa*-Tomato mice to lineage trace Nestin$^+$ cells more efficiently (based on *Nestin* mRNA levels in fetal and postnatal ovaries; *SI Appendix*, Fig. S1*H*). We first examined ovaries immediately after 4-OHT injection (24 h postinjection) to determine which Nestin$^+$ cells were initially labeled with Tomato. In E15.5- and E18.5-injected fetal ovaries, Tomato$^+$ cells were spindle-shaped cells adjacent to blood vessels that did not coexpress FOXL2 at E16.5 and P1, respectively (Fig. 2 *C*, *D*, *G*, and *H*). At P3 and P5 (in P2- and P4-injected ovaries, respectively), a small number of round-shaped Tomato-labeled cells coexpressed FOXL2, but the vast majority of initially labeled Tomato$^+$ cells were spindle-shaped FOXL2$^-$ cells specifically localized adjacent to vasculature (Fig. 2 *E–H*). The number of Tomato$^+$ cells consistently increased between fetal and postnatal stages (Fig. 2*G*), consistent with the idea that additional Nestin$^+$ cells are constantly recruited during ovarian differentiation.

Similar to E12.5 injection, ovaries exposed to 4-OHT at E15.5 showed only one to two follicles in each section containing Tomato-labeled FOXL2$^+$ cortical granulosa cells at P30 and P60 (Fig. 3 *A* and *B* and *SI Appendix*, Fig. S4 *A* and *B*). Additionally, we observed only a few Tomato$^+$ cells that expressed HSD3B1, a marker of thecal and interstitial steroidogenic cells in the adult ovarian stroma (30), in P30 and P60 samples (*SI Appendix*, Fig. S5 *A*, *B*, and *Y*). We also saw occasional Tomato$^+$ vascular smooth muscle cells (VSMCs) expressing alpha-smooth muscle actin (ACTA2; also called α-SMA) and pericytes expressing CSPG4 in the theca layer of follicles (31–34) in P30 and P60 ovaries that were exposed to 4-OHT at E15.5 (*SI Appendix*, Fig. S5 *C–F* and *Y*).

However, after administering 4-OHT to E18.5 ovaries, which mainly contained germline cysts at that stage, Tomato$^+$ cells were observed in a larger subset of granulosa cells of cortical follicles (Fig. 3 *C* and *D* and *SI Appendix*, Fig. S4 *C* and *D*). According to follicle quantification data, progeny of Nestin$^+$ cells in E18.5 fetal ovaries were biased toward granulosa cells in secondary-wave follicles (i.e., observed more often at P60 versus P30) (Fig. 3*I*). Only a few Tomato$^+$ cells expressed HSD3B1 at P30 (*SI Appendix*, Fig. S5 *G* and *Y*), whereas a larger number of Tomato$^+$ cells colocalized with HSD3B1 at P60 (*SI Appendix*, Fig. S5 *H* and *Y*). In P30 and P60 ovaries, many Tomato$^+$ cells were observed in the theca layer, expressing ACTA2 or CSPG4 (*SI Appendix*, Fig. S5 *I–L* and *Y*).

After administering 4-OHT at P2 (when germline cysts break apart and individual oocytes become surrounded by

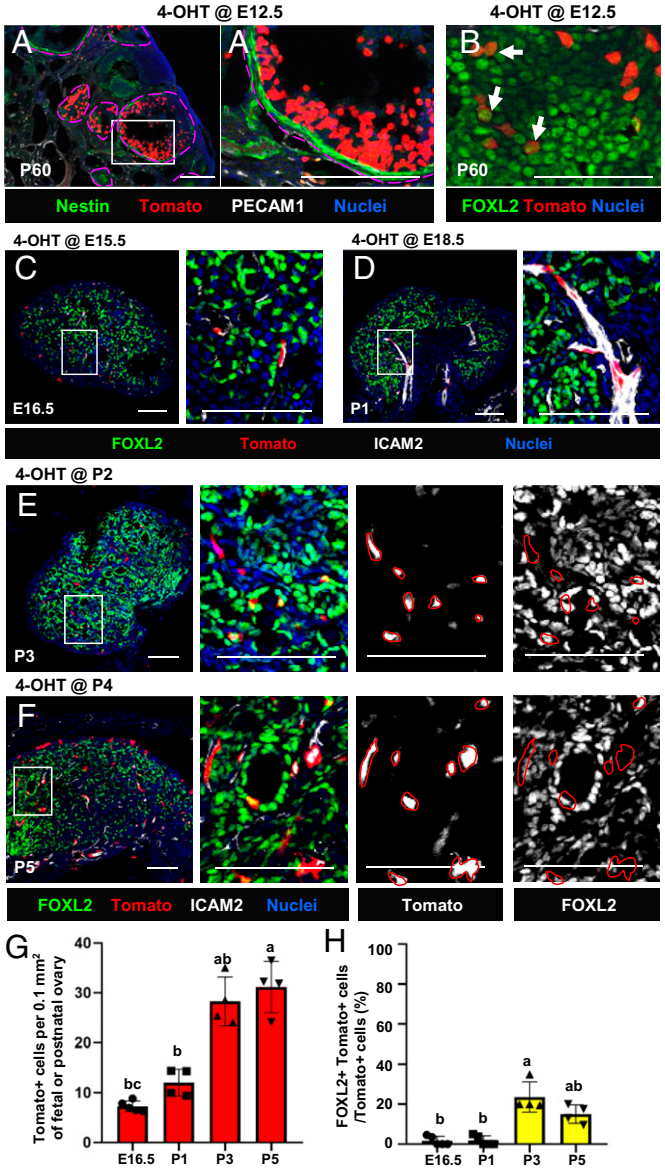

Fig. 2. Initial labeling in *Nestin*-CreER–mediated lineage tracing of fetal and postnatal ovaries is targeted to perivascular cells with minimal granulosa cell labeling. (*A* and *B*) Long-term lineage-tracing of P60 *Nestin*-CreER;*Rosa*-Tomato ovaries exposed to 4-OHT at E12.5. Arrows indicate Tomato$^+$ cells coexpressing FOXL2. (*C*–*F*) *Nestin*-CreER;*Rosa*-Tomato fetal and postnatal ovaries exposed to 4-OHT at E15.5 (*C*), E18.5 (*D*), P2 (*E*), and P4 (*F*). Images were taken 24 h after 4-OHT injection to determine initial Tomato reporter labeling. (Scale bars: 50 μm.) (*G* and *H*) Quantification (mean ± SD) of Tomato$^+$ cell number (*G*; $n = 5$ for E16.5 and $n = 4$ for P1, P3, and P5) and percentage of Tomato$^+$ cells coexpressing FOXL2 (*H*). Letters indicate statistical differences ($P < 0.05$).

somatic cells to form primordial follicles), more Tomato$^+$ cells overlapped with FOXL2 as compared to E18.5 injection (Fig. 3 *E*, *F*, and *I*). Additionally, Tomato$^+$ cells coexpressed CSPG4 and ACTA2 (markers of theca cells), as well as HSD3B1 (*SI Appendix*, Fig. S5 *M*–*R* and *Y*).

When pups were administered 4-OHT at P4, fewer Tomato$^+$ cells were FOXL2$^+$ granulosa cells in adult ovaries, while many Tomato$^+$ cells were interstitial mesenchymal cells (Fig. 3 *G* and *H* and *SI Appendix*, Fig. S4 *G* and *H*). Nestin$^+$ cells in P4 ovaries mainly contributed to granulosa cells in medullary first-wave follicles (Fig. 3*I*). Few Tomato$^+$ cells expressed HSD3B1 at P30; more Tomato$^+$ cells expressed HSD3B1 in P60 ovaries as compared to P2 injection (*SI Appendix*, Fig. S5 *S*, *T*, and *Y*). Likewise, Tomato$^+$ cells were observed in the theca layer (*SI Appendix*, Fig. S5 *U*–*X* and *Y*). Overall, lineage-tracing assays revealed that the contribution of Nestin-derived progenitors to interstitial ovarian lineages consistently increased between fetal and postnatal stages, by which point Tomato$^+$ cells labeled at P4 contributed to a majority of HSD3B1$^+$, ACTA2$^+$, and CSPG4$^+$ cells in the P60 ovary (*SI Appendix*, Fig. S5 *Y*).

The percentage of follicles with Tomato$^+$ granulosa cells in *Nestin*-CreER;*Rosa*-Tomato ovaries (exposed to 4-OHT at different stages) showed that P2-derived Nestin$^+$ cells contributed to granulosa cells in both first- and second-wave follicles (Fig. 3*I*), whereas P4-derived cells were less likely to give rise to granulosa cells in second-wave follicles and more likely to give rise to interstitial cell types such as steroidogenic cells in P60 ovaries. These data provide evidence that fetal and early postnatal Nestin$^+$ cells can give rise to granulosa cells, as well as theca cells and interstitial steroidogenic cells, in a stage-specific manner.

Maintenance of Nestin-Expressing Cells Requires Blood Vessels. To explore the requirement of vasculature for Nestin expression in fetal and postnatal ovaries, we disrupted vasculature ex vivo with a VEGF signaling blocker (VEGF receptor inhibitor VEGFR-TKI II). VEGFR-TKI II treatment significantly reduced expression of the endothelial-specific markers ICAM2 and *Cdh5* (Fig. 4 *A* and *B*), demonstrating the effectiveness of vascular

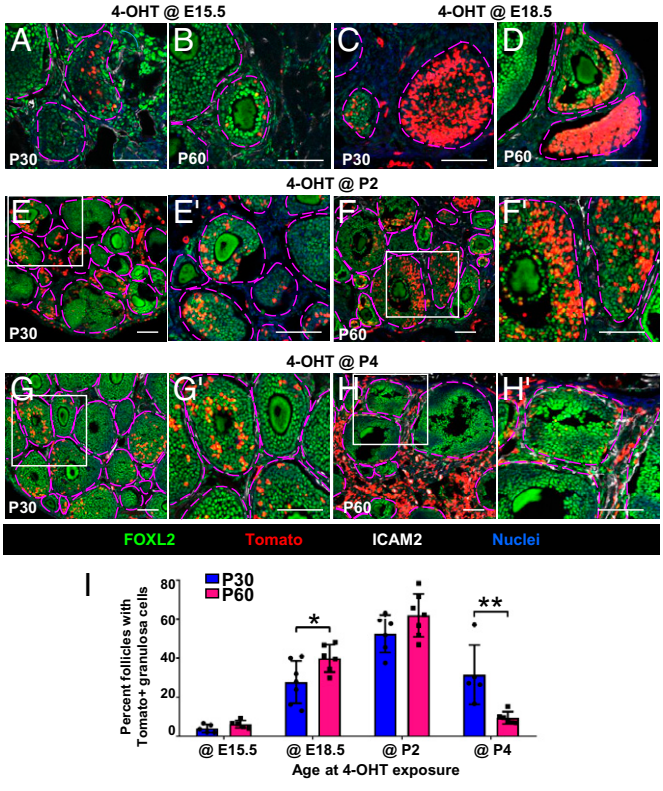

Fig. 3. Fetal and postnatal perivascular Nestin$^+$ cells give rise to adult granulosa cells. (*A*–*H*) Long-term lineage tracing of fetal and postnatal Nestin$^+$ cells in P30 (*A*, *C*, *E*, and *G*) and P60 (*B*, *D*, *F*, and *H*) *Nestin*-CreER;*Rosa*-Tomato ovaries exposed to 4-OHT at E15.5 (*A* and *B*), E18.5 (*C* and *D*), P2 (*E* and *F*), or P4 (*G* and *H*). *E*′–*H*′ are higher-magnification images of the boxed regions in *E*–*H*. Ovarian follicles are outlined by magenta dashed lines. (Scale bars: 50 μm.) (*I*) Graph shows percentage (mean ± SD) of primary, secondary, and antral follicles containing Tomato$^+$ granulosa cells in P30 and P60 *Nestin*-CreER;*Rosa*-Tomato ovaries exposed to 4-OHT at E15.5 ($n = 5$ for P30 and P60), E18.5 ($n = 7$ for P30 and $n = 6$ for P60), P2 ($n = 6$ for P30 and $n = 7$ for P60), or P4 ($n = 5$ for P30 and $n = 6$ for P60). *$P < 0.05$, **$P < 0.01$.

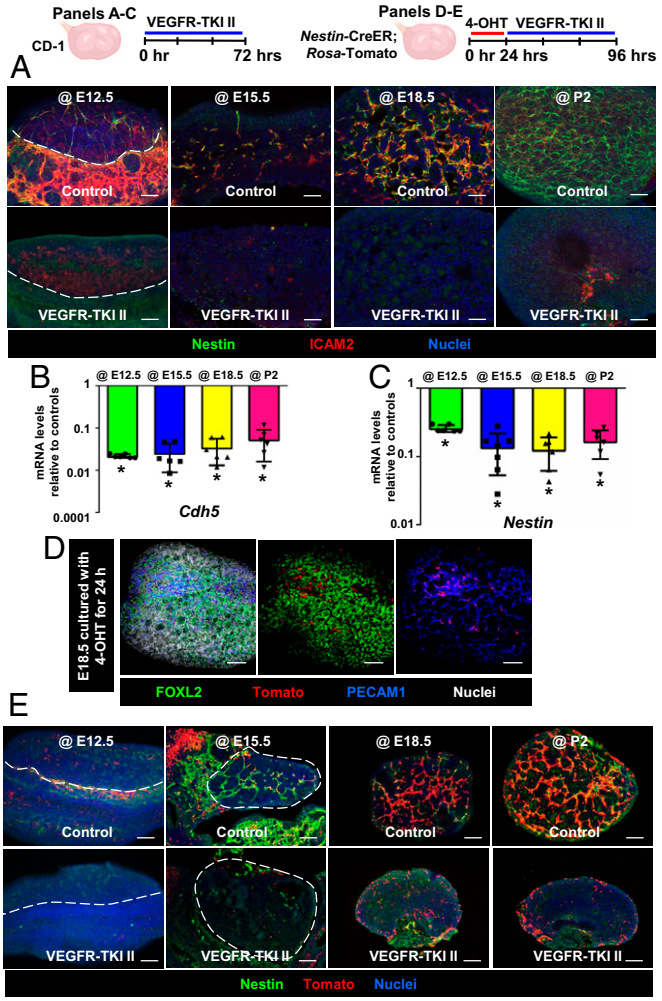

Fig. 4. Vasculature is required for maintenance of medullary perivascular Nestin$^+$ cells. (*A–C*) Immunofluorescence images (*A*) and qRT-PCR analyses (mean ± SD) (*B* and *C*) of E12.5, E15.5, E18.5, or P2 wild-type CD-1 ovaries ($n = 6$) cultured ex vivo with DMSO (control) or VEGFR-TKI II (VEGFR inhibitor). *$P < 0.05$. (*D*) E18.5 *Nestin*-CreER;*Rosa*-Tomato fetal ovary after 24-h ex vivo exposure to 4-OHT. (*E*) Ex vivo vascular disruption of *Nestin*-CreER; *Rosa*-Tomato cultured fetal and postnatal ovaries after initial exposure to 4-OHT for 24 h. Dashed lines indicate gonad–mesonephros border or gonad boundary. (Scale bars: 50 μm.)

inhibition. We also observed a reduction in mRNA and protein levels of *Nestin* (Fig. 4 *A* and *C*), indicating that ovarian *Nestin* expression is dependent on the presence of blood vessels.

To directly visualize whether Nestin-derived cells remained in the ovary in the absence of vasculature, we disrupted vasculature ex vivo in *Nestin*-CreER;*Rosa*-Tomato fetal and postnatal ovaries, in which Nestin-derived cells and their progeny are permanently labeled (Fig. 4*D*). We first addressed whether cells labeled ex vivo were perivascular cells and not surface epithelial or other cell types; examination of gonads 24 h after exposure to 4-OHT showed that Tomato$^+$ cells were almost exclusively perivascular cells adjacent to blood vessels, with very rare surface epithelial cells labeled (Fig. 4*D*). Tomato$^+$ cells were no longer detectable after disruption of vasculature at E12.5. In E15.5 cultured fetal ovaries, some Tomato-labeled cells, which had a different cellular morphology as compared to controls, remained in the vascular-disrupted gonads. Most spindle-shaped Tomato$^+$ cells in control ovaries were next to blood vessels in the medullary region; however, after vascular disruption at E18.5, Tomato$^+$ cells changed from spindle shaped into round shaped, and they were enriched in the ovarian cortex relative to controls. Ablation of vasculature in P2 cultured ovaries also resulted in the reduction of medullary (perivascular) Tomato-labeled cells and also increased the number of Tomato$^+$ cortical cells (Fig. 4*E*).

Vasculature Is Required to Maintain Undifferentiated Perivascular Nestin-Derived Cells. We next used *Nestin*-CreER;*Rosa*-Tomato ovaries to examine the specific fate of Nestin-derived cells after vascular disruption. As expected, VEGFR-TKI II significantly decreased ICAM2 expression (Fig. 5 *A–C*). Whereas E15.5, E18.5, and P2 control cultured ovaries contained Tomato$^+$ spindle-shaped perivascular cells, Tomato$^+$ cells that remained in vascular-disrupted ovaries were cortical FOXL2$^+$ cells (Fig. 5 *A–D*). These data indicated that the disruption of vasculature induced differentiation of perivascular Nestin$^+$ cells into FOXL2$^+$ pregranulosa cells.

Even though Tomato$^+$ cells expressed FOXL2 after vascular disruption, the total number of Tomato$^+$ cells was reduced compared to controls (Fig. 5 *A–C*). To address whether reduced Tomato$^+$ cell number was due to apoptosis (as opposed to reduced *Nestin* expression and subsequent reduced *Nestin*-CreER activity), we assessed cleaved Caspase-3 expression. We observed that vascular disruption induced cleaved Caspase-3 expression and some Tomato$^+$ cells coexpressed cleaved Caspase-3 at E15.5, suggesting that reduction of Tomato$^+$ cells was at least partly due to apoptosis after vascular disruption (*SI Appendix*, Fig. S6*A*). Taken together, these data suggest that vasculature is required to maintain perivascular Nestin-derived cells in an undifferentiated state, prevent their differentiation into pregranulosa cells during a specific time window, and promote their survival.

To determine the effect of vascular disruption on other general cell lineages of the ovary, we assessed expression levels of *Nr5a1* and *Wt1* mRNA and protein in VEGFR-TKI-II–treated ovaries. By immunofluorescence, we did not observe any gross changes in the number or appearance of NR5A1$^+$ and WT1$^+$ cells in E15.5 and E18.5 cultured ovaries (*SI Appendix*, Fig. S6 *B* and *C*). qRT-PCR analyses revealed that there was a reduction in *Nr5a1* mRNA levels, but *Wt1* was unaffected (*SI Appendix*, Fig. S6*D*), indicating that there may be some specific effects on the NR5A1$^+$ lineage, to which perivascular cells belong, but not to the general WT1$^+$ ovarian somatic lineage.

Active Notch Signaling in Female Gonads Is Dependent on Vasculature. Active Notch signaling within fetal ovaries is restricted to somatic cells (35); however, it is unknown whether Notch signaling acts as the bridge between vasculature and somatic cells in fetal ovaries. To investigate Notch signaling activity in fetal and postnatal ovaries, we performed immunofluorescence analyses using a *CBF*:H2B-Venus Notch reporter mouse line, in which the activation of Notch signaling is reflected by the expression of Venus protein (36). In E15.5 female gonads, Notch activity was regularly observed in Nestin$^+$ cells; however, more perivascular Nestin$^+$ cells expressed Venus at E18.5 and P2 (*SI Appendix*, Fig. S7*A*). In P4 ovaries, Notch activity was much less frequently observed in perivascular Nestin$^+$ somatic cells (*SI Appendix*, Fig. S7*A*). Relative to E12.5 ovaries, mRNA levels of the Notch target genes *Hes1*, *Heyl*, and *Hey1* were up-regulated at E18.5 and peaked at P1, whereas mRNA levels of *Hes5* were slightly up-regulated and then were significantly reduced after birth (*SI Appendix*, Fig. S7 *B–E*). Taken together, Notch signaling was most active in the ovary between E18.5 and P2.

To determine whether pregranulosa cells underwent active Notch signaling, we examined FOXL2 expression in P2

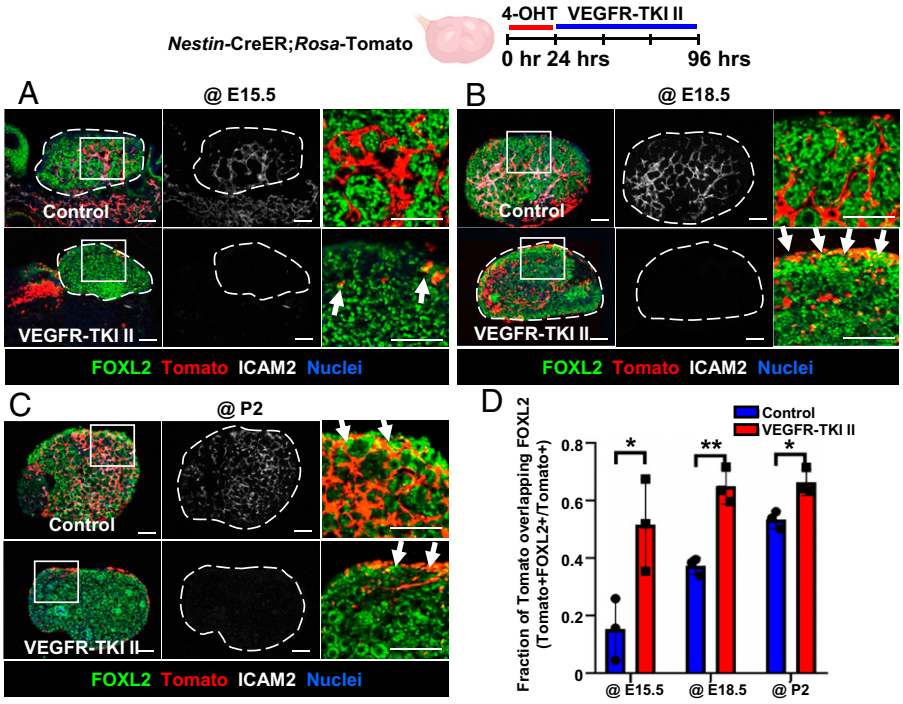

Fig. 5. Vascular disruption results in differentiation of Nestin$^+$ cells into cortical pregranulosa cells. Immunofluorescence images (*A–C*) and qRT-PCR analyses (mean ± SD) (*D*) of E15.5 (*A*), E18.5 (*B*), or P2 (*C*) *Nestin*-CreER;*Rosa*-Tomato ovaries cultured ex vivo with DMSO (control) or VEGFR-TKI II. Arrows throughout indicate Tomato$^+$/FOXL2$^+$ cells. Dashed outlines in *A–C* indicate gonad boundary. The *Rightmost* image in each panel is a higher-magnification image of the boxed region in the *Leftmost* image. (Scale bars: 50 μm.) (*D*) Fraction of Tomato expression overlapping with FOXL2 in different stages of ex vivo cultured ovaries ($n = 3$). *$P < 0.05$, **$P < 0.01$.

CBF:H2B-Venus ovaries. Immunofluorescence analyses showed that perivascular Venus$^+$ cells did not express FOXL2; however, some Venus$^+$ cells in the ovarian cortex that were not adjacent to vasculature coexpressed FOXL2 (*SI Appendix*, Fig. S7*F*). According to a previous scRNA-seq study, *Notch2* was highly expressed in pregranulosa cells (7), implicating NOTCH2 as a potential Notch receptor involved in this process. To determine whether NOTCH2-mediated signaling occurred in Nestin$^+$ cells, we used *Notch2*-ICD-Cre;*Rosa*-YFP embryos, in which active NOTCH2 signaling induces Cre activity (37) and permanently labels NOTCH2-activated cells and their progeny. We observed that Nestin$^+$ cells were labeled with YFP in E18.5 fetal ovaries (*SI Appendix*, Fig. S8*A*), demonstrating that fetal Nestin$^+$ cells underwent active NOTCH2-mediated signaling. We also examined the expression of DLL4, a potential ligand for NOTCH2, in fetal ovaries, and observed it was specifically expressed in the ovarian vasculature (*SI Appendix*, Fig. S8*B*).

To further analyze blood vessel control of Notch activity, we disrupted vasculature ex vivo in *CBF*:H2B-Venus fetal and postnatal ovaries. In E12.5 and E15.5 cultured fetal ovaries, Venus expression was absent in gonads after vascular disruption, while some Venus remained in the mesonephros (Fig. 6 *A* and *B*). At E18.5, blockade of vasculature resulted in a reduction of cortical Venus and absence of medullary Venus expression (Fig. 6*C*). However, vascular inhibition in P2 ovaries only disrupted active Notch signaling in the medulla and did not affect Notch activity in the cortex (Fig. 6*D*). Next, we examined mRNA levels of Notch target genes to further verify the role of the vasculature in driving active Notch signaling. *Hes1*, *Hes5*, *Hey1*, and *Heyl* mRNA levels were all significantly decreased after disruption of vasculature at E12.5, E15.5, and E18.5, but not at P2 (Fig. 6*E*).

Notch Signaling Regulates Differentiation of Ovarian Nestin$^+$ Progenitors. Whether Notch signaling is a critical aspect of vascular–mesenchymal interactions during ovarian differentiation in this context has not been definitively assessed. Specifically, we hypothesized that Notch signaling is responsible for the maintenance of ovarian perivascular Nestin$^+$ cells; thus, we blocked Notch activity by using the γ-secretase inhibitor N-[N-(3,5-difluorophenacetyl-L-alanyl)]-(S)-phenylglycine t-butyl ester (DAPT) in fetal and postnatal ovaries ex vivo. Expression of Notch target genes was significantly reduced in DAPT-treated groups, demonstrating that Notch signaling was effectively blocked (Fig. 7*A*). Blockade of Notch activity reduced Nestin protein expression in E15.5, E18.5, and P2 cultured ovaries (Fig. 7 *B–D*). However, DAPT also decreased ICAM2 expression at E18.5 and P2 (Fig. 7 *C* and *D*), indicating a disruption in vasculature. We next examined *Nestin* and *Cdh5* mRNA levels in DAPT-treated ovaries. *Nestin* was significantly down-regulated by DAPT at E15.5, E18.5, and P2 (Fig. 7*E*). Similar to immunofluorescence analyses, DAPT only affected *Cdh5* at E18.5 and P2 but not at E15.5 (Fig. 7*F*), indicating there is a stage-specific effect of Notch signaling upon ovarian vascular development. To determine whether the reduction of *Nestin* in DAPT-treated ovaries was due to disruptions of vascular differentiation and down-regulation of *Cdh5* mRNA expression, we treated E18.5 ovaries with DAPT for 12, 18, or 24 h. DAPT specifically decreased *Nestin* mRNA levels when cultured for 18 h (i.e., did not significantly affect *Cdh5* levels) (*SI Appendix*, Fig. S8*C*), suggesting that disruption of *Nestin* expression preceded any vascular disruption, and that reduction of *Nestin* expression by DAPT is not solely due to a potential reduction in vascular endothelial cells.

To examine the fate of Nestin$^+$ cells after blockade of Notch signaling, we inhibited Notch activity in *Nestin*-CreER;*Rosa*-Tomato ovaries via DAPT treatment ex vivo (Fig. 7*G*). In E15.5 cultured ovaries, DAPT treatment reduced the number of Tomato$^+$ cells, which did not express FOXL2. Similar to vascular disruption, in E18.5 and P2 DAPT-cultured ovaries we saw that medullary perivascular Tomato$^+$ cells were decreased while FOXL2$^+$/Tomato$^+$ cells were enriched in the ovarian cortex (Fig. 7 *G* and *H*). Our data suggest that blockade of Notch signaling induced the differentiation of Nestin$^+$ cells into cortical pregranulosa cells and reduced medullary perivascular undifferentiated Nestin$^+$ cells. Furthermore, while

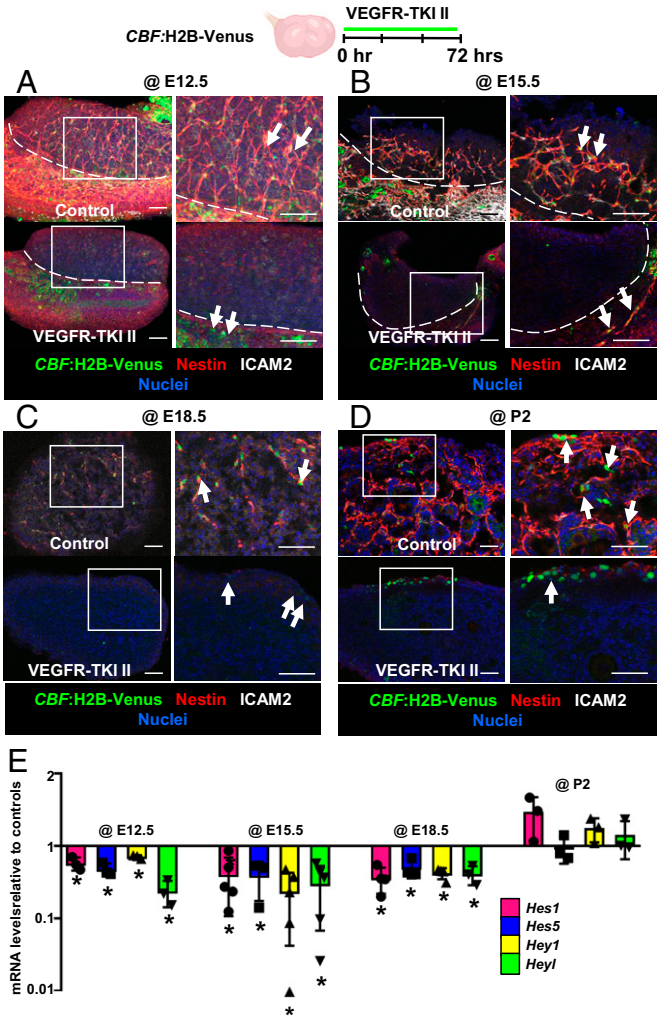

Fig. 6. Vasculature is essential for medullary Notch activity in fetal and postnatal ovaries. Immunofluorescence images (*A–D*) and qRT-PCR analyses (mean ± SD) (*E*) of E12.5 (*A*), E15.5 (*B*), E18.5 (*C*), or P2 (*D*) *CBF*:H2B-Venus ovaries (Notch signaling reporter) cultured ex vivo with DMSO (control) or VEGFR-TKI II. Arrows throughout indicate Venus$^+$ cells in the gonad or mesonephros. The image on the *Right* in each panel is a higher-magnification image of the boxed region in the *Left* image. Dashed lines in *A* and *B* indicate gonad–mesonephros border. (Scale bars: 50 μm.) (*E*) qRT-PCR analyses showing fold change in Notch target gene (*Hes1*, *Hes5*, *Hey1*, and *Heyl*) mRNA levels after disruption of vasculature in E12.5, E15.5, E18.5, or P2 cultured CD-1 ovaries ($n = 3$). *$P < 0.05$.

Notch activity depended on vasculature in earlier fetal stages, active Notch signaling might contribute to vascular formation in later stages.

To address whether Notch signaling is specifically required in perivascular cells to maintain their undifferentiated status in the ovary, we performed a cell-type–specific conditional deletion of the Notch transcriptional regulator *Rbpj* (also known as *Cbf1*) within permanently labeled Nestin-derived cells using a *Nestin*-CreER;*Rosa*-Tomato;*Rpbj*-flox/flox mouse model. As expected, Tomato$^+$ cells in control *Nestin*-CreER;*Rosa*-Tomato; *Rpbj*-flox/+ heterozygous control littermate ovaries were overwhelmingly perivascular, undifferentiated, and FOXL2$^-$ (Fig. 8 *A* and *B*). In contrast, Tomato$^+$ cells in *Nestin*-CreER; *Rosa*-Tomato;*Rpbj*-flox/flox ovaries were nearly all FOXL2$^+$ and no longer strictly perivascular localized (Fig. 8 *A* and *B*). Similar to ex vivo DAPT culture results, in vivo deletion of *Rbpj* in Nestin-expressing cells at P2 also reduced perivascular Tomato$^+$ cells (Fig. 8*C*). However, some Tomato$^+$ cells remained adjacent to vasculature, suggesting that some postnatal perivascular cells were not controlled by Notch signaling. These data definitively demonstrate that Notch signaling is required within perivascular cells to prevent them from differentiating into FOXL2$^+$ granulosa cells during a specific time window.

Nestin$^+$ Cells Are Required for Folliculogenesis. If perivascular Nestin$^+$ cells represent pregranulosa progenitors, we anticipated that ablating these cells would compromise granulosa cell differentiation or follicular development during ovary organogenesis. To specifically deplete Nestin$^+$ progenitors from the ovary, we used a Cre-responsive *Rosa*-diphtheria toxin A (DTA) mouse line (38) driven by *Nestin*-CreER in which diphtheria toxin is only expressed in CreER-active cells, thus inducing apoptosis only in perivascular cells. We injected 4-OHT to deplete Nestin$^+$ cells at P2 and P4 (Fig. 9*A*), at the stages with highest ovarian *Nestin* expression. Compared with *Nestin*-CreER;*Rosa*-Tomato controls lacking *Rosa*-DTA, Tomato expression was absent in P7 and P21 *Nestin*-CreER; *Rosa*-Tomato;*Rosa*-DTA ("DTA$^+$") ovaries, indicating efficient ablation of Nestin$^+$ cells (*SI Appendix*, Fig. S9 *A* and *B*).

We then assessed how the loss of Nestin$^+$ perivascular cells affected ovarian morphology and histology. At P7, when control follicles normally contain single oocytes, in DTA$^+$ ovaries some abnormal oocyte cysts containing multiple germ cells (i.e., polyovular follicles) remained in the medulla, and more oocyte cysts were observed in the cortex (Fig. 9 *B* and *C*), indicative of defective or delayed oocyte cyst breakdown. We next classified and counted follicles (primordial, primary, secondary, and antral follicles) according to established morphological criteria (39). Total follicle number in P7 DTA$^+$ ovaries was similar compared to control ovaries; however, Nestin-cell–depleted ovaries exhibited a significantly reduced number of primary follicles, while numbers of primordial and secondary follicles were unchanged at P7 (Fig. 9*D*).

While control P21 ovaries exhibited normal, ongoing follicular progression, DTA$^+$ ovaries contained numerous polyovular ovarian follicles and exhibited defects in folliculogenesis, showing a significantly reduced number of antral follicles as compared to controls (Fig. 9 *E–G*). Some polyovular follicles were observed in P21 control ovaries, which might be an effect of postnatal 4-OHT injection, but at a rate significantly lower than DTA$^+$ ovaries (Fig. 9*F*). To address whether any disruptions in vascular development could have contributed to this phenotype, we examined blood vessels in control versus DTA$^+$ P21 ovaries; however, PECAM1 staining revealed similar blood vessel patterns in perifollicular and interstitial regions of the ovary in both groups (*SI Appendix*, Fig. S9*C*). While polyovular follicles were not detected in P60 DTA$^+$ ovaries (*SI Appendix*, Fig. S9*D*), the numbers of total follicles and antral follicles were significantly reduced in P60 DTA$^+$ ovaries (*SI Appendix*, Fig. S9*E*), suggesting that polyovular follicles underwent apoptosis. Overall ovary size was also reduced (*SI Appendix*, Fig. S9*D*), likely caused by a reduction in interstitial cell populations. Overall, our data suggest that depletion of postnatal Nestin$^+$ perivascular cells caused disruptions in ovarian development and demonstrate that perivascular cells are essential for the breakdown of germline cysts and subsequent follicular formation.

Discussion

In the adult human ovary, de novo angiogenesis composed of endothelial and perivascular cells occurs in the theca layer of

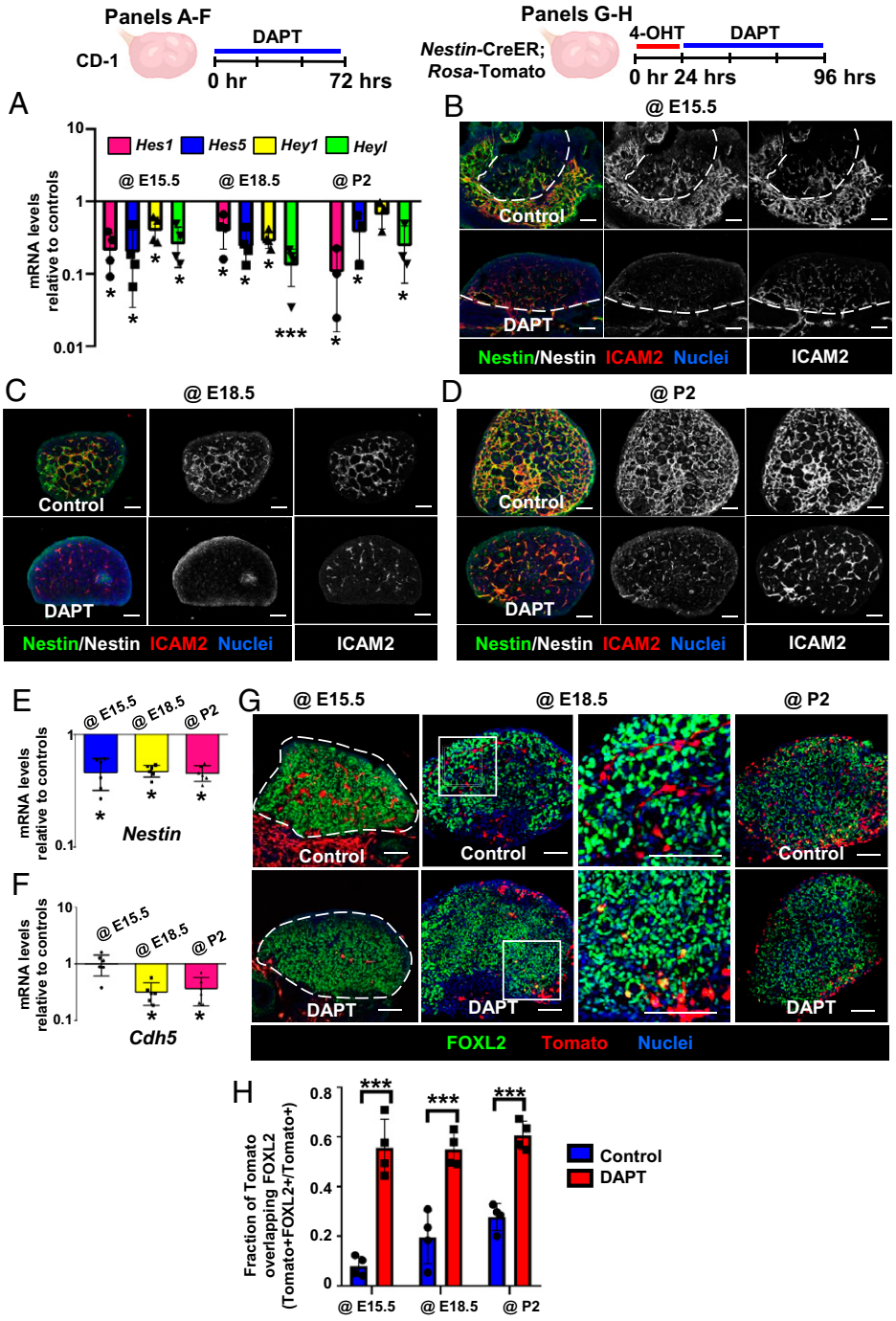

Fig. 7. Disruption of Notch signaling induces differentiation of Nestin-derived cells into pregranulosa cells. (*A–F*) qRT-PCR analyses (mean ± SD) (*A*, *E*, and *F*) (n = 3 to 4 for *A*; n = 6 for *E* and *F*) and immunofluorescence images (*B–D*) of E15.5 (*B*), E18.5 (*C*), or P2 (*D*) CD-1 ovaries cultured ex vivo with DMSO (control) or DAPT (Notch signaling inhibitor). (*G*) Ex vivo culture of E15.5, E18.5, or P2 *Nestin*-CreER;*Rosa*-Tomato fetal and postnatal ovaries. *Right* image for @E18.5 samples is a higher-magnification image of the boxed region in the *Left* image. Dashed lines throughout indicate gonad outline or border. (Scale bars: 50 μm.) (*H*) Fraction of Tomato expression overlapping with FOXL2 (mean ± SD) in different stages of ex vivo cultured ovaries (n = 3). *P < 0.05, ***P < 0.001.

follicles in the early process of follicular growth (40). Additionally, around 10% of human ovarian cortex cells were annotated as perivascular cells in a recent single-cell study (18); however, the functional roles of vasculature and perivascular cells in ovarian function are not fully understood. Thus, addressing the roles of perivascular cells is essential for understanding the mechanisms underlying ovarian development. In this study, we identify Nestin$^+$ cells as a source of cortical granulosa cells that are maintained in a perivascular niche via vascular-mediated Notch signaling. Strikingly, depletion of Nestin$^+$ cells in postnatal ovaries impaired the breakdown of germline cysts and disrupted follicular development, likely due to insufficient pregranulosa cells to surround individual oocytes. Our findings in this study thus reveal a critical functional role of vasculature and perivascular cells in supporting folliculogenesis.

Nestin is a marker of stem cells in many tissues, including the testis (14, 25, 41), in which Nestin$^+$ cells are putative progenitors for fetal Leydig cells and adult Leydig cells (14, 25). In ovaries, Nestin induced by a luteinizing hormone (LH) surge via VEGF signaling promotes angiogenesis in the follicle (42), but Nestin$^+$ cells' specific roles in the ovary were unclear, representing a major outstanding question in the field. Here, we demonstrate that perivascular Nestin$^+$ cells are bona fide cortical granulosa cell progenitors, thus uncovering a cellular source for granulosa cells.

A common belief is that Sertoli cells and granulosa cells arise from a common cell lineage in the gonadal primordium (43, 44). Our lineage-tracing experiments here showed that ovarian Nestin$^+$ cells gave rise to granulosa cells. However, we previously reported that testicular Nestin$^+$ cells do not give rise to Sertoli cells (14). We also previously showed that testicular

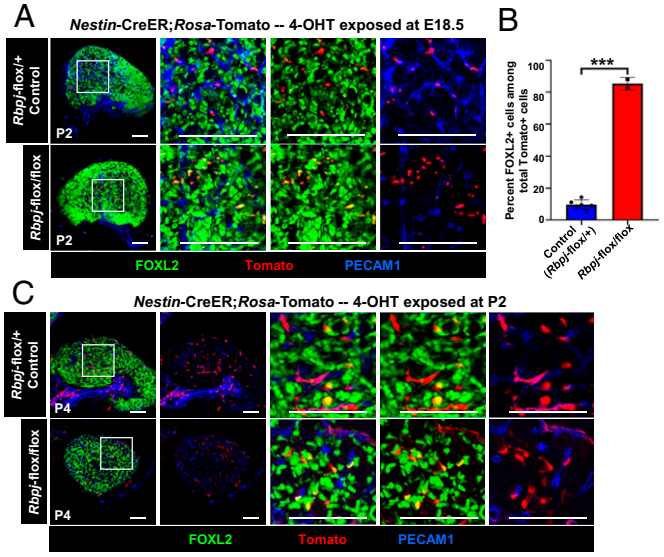

Fig. 8. Conditional disruption of Notch signaling specifically in Nestin$^+$ cells results in differentiation of Nestin-derived cells into pregranulosa cells. Immunofluorescence images of P2 (*A*) and P4 (*C*) *Nestin*-CreER;*Rosa*-Tomato;*Rbpj*-flox/+ heterozygous control (*Top*) and *Nestin*-CreER;*Rosa*-Tomato;*Rbpj*-flox/flox (*Bottom*) postnatal ovaries exposed to 4-OHT at E18.5 and P2, respectively. (*B*) Graph shows percentage of FOXL2-expressing cells among Tomato$^+$ cells (mean ± SD) in P2 control ($n = 6$) and *Rbpj* conditionally deleted ovaries ($n = 3$) exposed to 4-OHT at E18.5. (Scale bars: 50 μm.) ***$P < 0.001$.

Nestin$^+$ cells are a WT1$^+$ progenitor population with a mesonephric origin (14), but in the female gonad, here we found that Nestin$^+$ cells are a NR5A1$^+$ gonadal mesenchymal population at early fetal stages. These results indicate that granulosa cells, in particular ones that arise later in development, and Sertoli cells do not strictly arise from a common precursor. In addition, in contrast to testicular Nestin$^+$ cells that possess self-renewal capacity to expand their numbers (14, 24), in the fetal ovary new Nestin$^+$ progenitors are instead continuously induced or recruited following blood vessels' ongoing formation. Moreover, whereas Sertoli cell precursors seem to be mostly derived during a tight time window from a single cellular source (i.e., coelomic epithelium) (45), granulosa cells in the ovary appear to have multiple origins and a wide developmental time window during which they are specified. These differences in gonadal supporting cell specification may be due to the inherent distinctions between spermatogenesis and oogenesis and the kinetics of germline–soma interactions in the testis versus ovary.

Our lineage-tracing assays showed different behaviors of Nestin$^+$ cells at different stages of ovary development. At E15.5, likely the developmental stage during which cortical granulosa cell progenitors begin to arise, Nestin$^+$ progenitors were only adjacent to blood vessels. Instead, most Nestin$^+$ granulosa progenitors emerged between E18.5 and P2, the time when germline cyst breakdown and formation of primordial follicles take place. This time window is likely when the maximum number of granulosa cells is needed to envelop individual oocytes completely and efficiently. In contrast, fewer granulosa cells arising from Nestin$^+$ progenitors at P4 could be observed. Since at P4 the formation of primordial follicles is almost complete (46) and there is no need for further granulosa cell specification, most Nestin$^+$ cells devoted to a granulosa cell fate have already differentiated and no longer express Nestin. Our long-term lineage tracing results showed that Nestin$^+$ cells present at P4 displayed multipotency and later in development differentiated into many different cell types, such as theca cells, pericytes, and interstitial steroidogenic cells, which are required after the establishment of primordial follicles is completed and the ovarian environment needs to be primed for follicular progression. This later in vivo multipotency is also a feature of testicular Nestin$^+$ cells (14) and reveals a similarity between Nestin$^+$ cells in the two sexes. However, we do add the caveat that these current findings can only support the idea that Nestin$^+$ cells are multipotent as a population of cells, as we were unable to address whether individual Nestin$^+$ cells themselves are multipotent.

The vasculature is intimately associated with maintenance and differentiation of Nestin$^+$ progenitors in the fetal testis (14), but vasculature's functional role, if any, in the ovary was as of yet unclear. Here we explored the mechanism of vascular–mesenchymal cross-talk in the developing ovary. We found that vascular disruption reduced the number of Nestin$^+$ progenitors, resulting in precocious or ectopic differentiation of Nestin$^+$ cells into FOXL2-expressing cortical pregranulosa cells. As a likely result, the reduction of progenitors in late fetal ovaries would likely lead to a subsequent deficit of pregranulosa cells, thus disrupting the kinetics and/or efficiency of folliculogenesis. Our *Nestin*-CreER;*Rosa*-DTA results support the idea that postnatal Nestin$^+$ cells participate in germline cyst breakdown and folliculogenesis. Similarly, knockout of *Foxl2* impairs germline cyst breakdown by apparently affecting the differentiation of granulosa cells and the disruption of the basal lamina surrounding follicles (47). However, depletion of LGR5$^+$ cells in fetal stages does not affect follicular assembly but rather the number of primordial follicles (7). Since LGR5 expression becomes limited to the ovarian surface epithelium in neonatal stages (48), and since most Nestin$^+$ cells emerged between E18.5 and P2, the time when germline cyst breakdown and formation of primordial follicles take place, we propose that FOXL2$^+$ and Nestin$^+$ granulosa progenitors are more essential for follicular assembly events. Therefore, depletion of Nestin$^+$ cells in postnatal ovaries likely resulted in a reduction of somatic cells surrounding the cysts, and they were subsequently unable to enclose individual oocytes, thus uncovering the importance of Nestin$^+$ progenitor cells during ovary development (Fig. 9*H*).

During ovarian organogenesis, Notch signaling directs the early stages of germline cyst breakdown and primordial follicle formation and maintenance (49, 50), likely by promoting the formation of primordial follicles via the regulation of oocyte survival and proliferation of pregranulosa cells (51). In contrast, Notch's role in the ovarian interstitium was unclear. Here we found that Notch activity was increased at E18.5, during the onset of germline cyst breakdown, consistent with studies of Notch family gene expression in the neonatal mouse ovary (49). However, we detected Notch activity within perivascular mesenchymal cells, implicating vasculature as a mediator of ovarian Notch signaling, which is an addition to the field.

While endothelial cells provide critical Notch ligands to perivascular Nestin$^+$ cells in the fetal testis (14), the importance of vasculature for Notch signaling in the developing ovary was unknown. The depletion of vasculature in *CBF*:H2B-Venus ovaries ex vivo showed that gonadal and medullary Notch activity, as well as Nestin expression, depends on the vasculature. However, the vasculature was also impaired by blocking Notch signaling at later stages, indicating that there are mutual or reciprocal effects of Notch on endothelial and mesenchymal cells: in early stages, activity of Notch depends on the vasculature, while later on, activation of Notch signaling might contribute to vasculature formation. Similar to vascular disruption, blockade of Notch signaling induced the ectopic or precocious differentiation of Nestin$^+$ cells into cortical pregranulosa cells

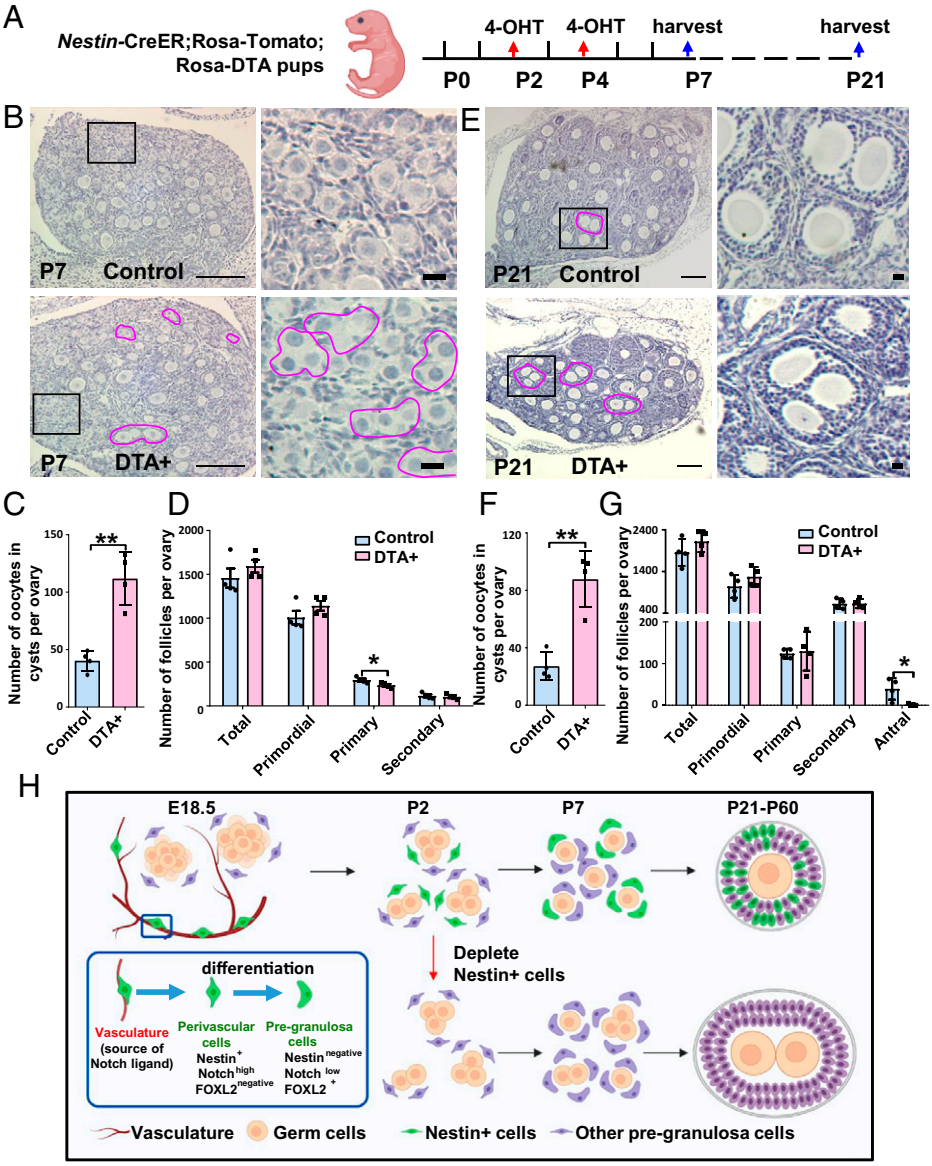

Fig. 9. Postnatal Nestin-derived cells are required for folliculogenesis. (*A*) Cartoon depicting experimental strategy for ablating postnatal Nestin$^+$ cells in *Nestin*-CreER; *Rosa*-Tomato;*Rosa*-DTA postnatal ovaries via exposure to 4-OHT at P2 and P4. (*B–G*) Hematoxylin staining (*B* and *E*), quantification of polyovular follicles (*C* and *F*), and follicle counts at different developmental stages (*D* and *G*) (mean ± SD) in *Nestin*-CreER; *Rosa*-Tomato;*Rosa*-DTA P7 (*B–D*) and P21 (*E–G*) ovaries. Magenta outlines denote polyovular follicles. $n = 4$ for each genotype and stage. $^*P < 0.05$, $^{**}P < 0.01$. (Thin scale bars: 50 μm; thick scale bars: 5 μm.) (*H*) Cartoon model depicting the dynamic marker expression pattern and function of Notch-signaling–regulated perivascular Nestin$^+$ cells in the ovary.

and reduced medullary perivascular undifferentiated Nestin$^+$ cells, thus revealing vasculature as a critical regulator of ovarian Notch activity. Later-stage Nestin-derived cells, which were largely fated to become interstitial cells, are likely regulated via non-Notch mechanisms, as we see a general down-regulation of Notch activity in later postnatal stages. Future analyses are needed to address the mechanisms regulating later-stage progenitor cells in the ovarian interstitium.

Fetal ovarian FOXL2$^+$ progenitors are well-characterized granulosa cell progenitors, which mainly contribute to granulosa cells in first-wave follicles (7, 52). Recently, fetal epithelial LGR5$^+$ cells were identified as a second class of granulosa cells in the ovary (7). However, not all granulosa cells in second-wave follicles arose from LGR5$^+$ progenitors, as shown by long-term lineage tracing experiments (6). Our study reveals a precursor of granulosa cells, perivascular Nestin$^+$ cells, which contribute to granulosa cells in both first- and second-wave follicles. In vivo cell ablation revealed a crucial role for Nestin$^+$ progenitors in the differentiation of pregranulosa cells, ensuring the timely and efficient formation of primordial follicles. Furthermore, our results show that the Nestin$^+$ population of cells is multipotent and gives rise to distinct cell types at different stages of development. Our data reveal how blood vessels mediate a balance between maintenance and differentiation of ovarian progenitors and their importance for folliculogenesis. These findings provide insights into ovarian organogenesis which may have implications for our understanding of the etiology of female gonad dysgenesis and infertility.

Materials and Methods

Mice. CD-1 mice (Charles River) were used for wild-type expression and ex vivo organ culture studies. Cre-responsive *Rosa*-Tomato [B6.Cg-*Gt(ROSA)26Sor*$^{tm14(CAG-tdTomato)Hze}$; JAX stock #007914], *Rosa*-DTA [*Gt(ROSA)26Sor*$^{tm1(DTA)Jpmb}$; JAX stock #009669], *Nr5a1*-Cre [Tg(Nr5a1-cre)7Lowl/J; JAX stock #012462], *Lgr5*-CreER [B6.129P2-Lgr5$^{tm1(cre/ERT2)Cle}$/J; JAX stock #008875], and *CBF*:H2B-Venus [Tg(Cp-HIST1H2BB/Venus)47Hadj; JAX stock #020942] mice were obtained from The Jackson Laboratory. *Nestin*-CreER mice [Tg(Nes-cre/ERT2,-ALPP)1Sbk] (14, 53) were obtained from Masato Nakafuku, Division of Developmental Biology, Cincinnati Children's Hospital Medical Center, Cinncinati, OH. *Notch2-ICD*-Cre mice (*Notch2*$^{tm2(cre)Rko}$) (37, 54) were used to lineage trace cells that underwent NOTCH2 signaling via a Cre-responsive Rosa-YFP reporter strain [*Gt(ROSA)26Sor*$^{tm3(CAG-EYFP)Hze}$/J; JAX stock #006148]; these strains were provided by Raphael Kopan, Division of Developmental Biology, Cincinnati Children's Hospital Medical Center via Joo-Seop Park, Divisions of

Pediatric Urology and Developmental Biology, Cincinnati Children's Hospital Medical Center. *Rbpj* floxed mice (*Rbpj*^{tm1Hon}) (55) were provided by Joo-Seop Park. Mice were housed in accordance with National Institutes of Health guidelines, and experimental protocols were approved by the Institutional Animal Care and Use Committee (IACUC) of Cincinnati Children's Hospital Medical Center (protocol #IACUC2021-0016).

Immunofluorescence. Tissues were fixed in 4% paraformaldehyde (PFA) with 0.1% Triton X-100 overnight at 4 °C. Whole-mount immunofluorescence was performed on gonads at stages E11.5–E13.5. After several washes in PBS + 0.1% Triton X-100 (PBTx), samples were incubated in blocking solution (PBTx + 10% fetal bovine serum [FBS] + 3% bovine serum albumin [BSA]) for 1 h at room temperature and incubated with primary antibodies (listed in *SI Appendix*, Table S1) overnight at 4 °C. After several washes in PBTx, samples were incubated in Alexa-488, Alexa-555, and Alexa-647 conjugated fluorescent secondary antibodies (Molecular Probes/Life Technologies/Thermo Fisher) and 2 μg/mL nuclear dye Hoechst 33342 (#H1399, Thermo Fisher) for 4 h rocking at room temperature, washed in PBTx, and mounted on slides in Fluoromount-G (SouthernBiotech).

For fetal ovaries at stages E15.5 and older, cryosections were performed. Samples were processed through a sucrose:PBS gradient (10, 15, 20% sucrose) before an overnight incubation in a 1:1 mixture of 20% sucrose and Optimal Cutting Temperature (OCT) medium (Sakura) rocking at 4 °C, then embedded in OCT medium. Cryosections (12 μm) were then stained and mounted as above, except secondary antibodies were applied for only 1 h.

Colocalization Analysis. Colocalization of FOXL2/HSD3B1/ACTA2/CSPG4 and Tomato was analyzed using the JACoP plugin in ImageJ. The plugin evaluated colocalization in two images according to M2 coefficients, which are defined as the ratio of the "summed intensities of pixels from the red image for which the intensity in the green channel is above zero" to the "total intensity in the red channel" (56).

Lineage Tracing of Nestin$^+$ Cells. After mating with *Nestin*-CreER males, pregnant *Rosa*-Tomato females were injected intraperitoneally with 75 μg/g 4-OHT (Sigma-Aldrich, #H6278) dissolved in corn oil. For E12.5 injection experiments, an additional progesterone (Sigma-Aldrich, #P0130; 37.5 μg/g) injection was given subcutaneously at E14.5 to help maintain pregnancy further after 4-OHT administration (14).

Ablation of Nestin$^+$ Cells. Control *Nestin*-CreER;*Rosa*-Tomato and cell-ablated *Nestin*-CreER;*Rosa*-Tomato;*Rosa*-DTA pups were intragastrically injected with 4-OHT (0.05 mg/each pup) at P2 and P4.

EdU Incorporation Assays. Pregnant mice received a single intraperitoneal injection of 50 mg/kg EdU (57). Four hours after EdU injection, fetal ovaries were collected. A Click-iT EdU Cell Proliferation Kit for imaging (#C10337, Thermo Fisher Scientific) was used.

MitoTracker Coelomic Epithelial Labeling. CD-1 gonads were incubated in 1 mM MitoTracker Orange CMTMRos (#M7510, Thermo Fisher Scientific/Invitrogen) in phosphate-buffered saline (PBS) for 30 min at 37 °C to label the surface epithelium. Following incubation with MitoTracker, gonads were washed several times in culture media. Gonads were then cultured for 48 h. As a control, several gonads in each experiment were removed and fixed immediately after labeling and washing with culture media to ensure that only the surface coelomic epithelial cells were initially labeled.

Flow Cytometry. Fetal ovaries were dissected and pooled in a 1.5-mL microcentrifuge tube. Ovaries were incubated in 0.05% trypsin-ethylenediaminetetraacetic acid (EDTA) (#25300054, Thermo Fisher Scientific/Gibco) at 37 °C for 6 min. Digestion was stopped with 10% FBS. Trypsin mixture was removed after centrifugation. One milliliter of 10% FBS solution (in 4 °C PBS) was added, and cells were kept on ice until flow cytometric analysis.

For perivascular and endothelial cell marker analyses, cells were fixed with 4% PFA for 15 min at 4 °C, washed with PBTx, and incubated with anti-CSPG4 and anti-PECAM1 antibodies for 15 min at 4 °C. Fluorescent secondary antibodies were applied for 15 min at 4 °C.

Histological Analysis of Ovaries and Follicle Quantification. Serial paraffin-embedded sections (5 μm) were deparaffinized and rehydrated through a series of xylene and ethanol. Sections were stained with hematoxylin (Denville). Follicles were counted in every fifth section through the entire ovary from each mouse as described previously (58). All follicle stages were categorized according to morphological criteria (39). For secondary to large antral follicles, we counted only follicles with a visible nucleus to avoid double counting. The total number of follicles was defined as the sum of the number of all stages of follicles in one ovary.

Ex Vivo Whole-Organ Ovarian Culture. Ovaries were cultured using an agar culture method as previously described (59). Briefly, organs were positioned on 1.5% agarose gel placed in Petri dishes with complete medium (Dulbecco's Modified Eagle Medium [DMEM]/10% FBS/1% penicillin–streptomycin) at 37 °C and 5% CO_2. 1.8 μg/mL VEGF Receptor Tyrosine Kinase Inhibitor II (VEGFR-TKI II; Calbiochem/EMD Millipore #676481-5MG) dissolved in dimethyl sulfoxide (DMSO) was used to disrupt blood vessels (60) and 100 μM γ-secretase inhibitor IX (DAPT; Calbiochem/EMD Millipore #565770-5MG) dissolved in DMSO was used to block γ-secretase activity (14). Wild-type CD-1 gonads were cultured for 72 h, whereas CreER embryos necessitating 4-OHT treatment were cultured for 96 h.

In *Nestin*-CreER;*Rosa*-Tomato ex vivo culture experiments, 4-OHT (0.02 mg/mL in ethanol) alone was added to the culture media for the first 24 h of culture to induce CreER activity. After 4-OHT was removed, VEGFR-TKI II or DAPT (or vehicle control) was added for the remaining additional 72 h of culture.

To distinguish cultured ovaries from ovaries developed in utero, in the text we used the word "cultured" after the stage at which the culture was started. In figure panels, we used the "@" symbol to denote cultured ovaries. Therefore, "@E15.5" indicates ovaries dissected at E15.5 and then cultured ex vivo, whereas "E15.5" indicates an ovary of that stage that had developed entirely in utero.

RNA Extraction and qRT-PCR. Total RNA was extracted from gonads (separated from mesonephroi) using a standard TRIzol (Thermo Fisher) and isopropanol precipitation protocol. cDNA synthesis was performed with 500 ng of total RNA, using an iScript cDNA synthesis kit (Bio-Rad). The cDNA was then subjected to qRT-PCR using the Fast SYBR Green Master Mix (Applied Biosystems/Thermo Fisher) on the StepOnePlus Real-Time PCR System (Applied Biosystems/Thermo Fisher). Primers used for qRT-PCR are listed in *SI Appendix*, Table S2. All reactions were run in triplicate. *Gapdh* was used as an internal normalization gene. Data from qRT-PCR was calculated relative to controls using the ΔΔCt method.

Statistical Analysis. All results are shown as mean ± SD. A two-tailed Student's *t* test was performed to calculate *P* values, in which $P < 0.05$ was considered statistically significant. Statistical analyses were performed using Prism version 5.0 (GraphPad). For immunofluorescence, EdU incorporation, flow cytometry, organ culture, and qRT-PCR assays, at least three independent experiments were performed and within each experiment multiple ovaries ($n \geq 3$) were used; specific sample sizes are described in the figure legends. Numbers for cell counting assays are listed in *SI Appendix*, Table S3.

Data, Materials, and Software Availability. All study data are included in the article and/or supporting information.

ACKNOWLEDGMENTS. We thank Drs. Masato Nakafuku, Rafael Kopan, and Joo-Seop Park for mice and Dr. Dagmar Wilhelm for anti-FOXL2 antibody. We would like to acknowledge the Research Flow Cytometry Core in the Division of Rheumatology at Cincinnati Children's Hospital Medical Center, supported by NIH S10OD023410. We acknowledge BioRender software (biorender.com) for the creation of figures. This work was supported by NIH (grants R35GM119458 and R01HD094698 to T.D.) and the Lalor Foundation (S.-Y.L.).

1. D. Wilhelm, S. Palmer, P. Koopman, Sex determination and gonadal development in mammals. *Physiol. Rev.* **87**, 1–28 (2007).
2. I. Stévant, S. Nef, Genetic control of gonadal sex determination and development. *Trends Genet.* **35**, 346–358 (2019).
3. P. Smith, D. Wilhelm, R. J. Rodgers, Development of mammalian ovary. *J. Endocrinol.* **221**, R145–R161 (2014).
4. J. Tu, A. H. Cheung, C. L. Chan, W. Y. Chan, The role of microRNAs in ovarian granulosa cells in health and disease. *Front. Endocrinol. (Lausanne)* **10**, 174 (2019).

5. L. Mork *et al.*, Temporal differences in granulosa cell specification in the ovary reflect distinct follicle fates in mice. *Biol. Reprod.* **86**, 37 (2012).
6. R. H. Rastetter *et al.*, Marker genes identify three somatic cell types in the fetal mouse ovary. *Dev. Biol.* **394**, 242–252 (2014).
7. W. Niu, A. C. Spradling, Two distinct pathways of pregranulosa cell differentiation support follicle formation in the mouse ovary. *Proc. Natl. Acad. Sci. U.S.A.* **117**, 20015–20026 (2020).
8. L. Ding, T. L. Saunders, G. Enikolopov, S. J. Morrison, Endothelial and perivascular cells maintain haematopoietic stem cells. *Nature* **481**, 457–462 (2012).
9. Q. Shen *et al.*, Adult SVZ stem cells lie in a vascular niche: A quantitative analysis of niche cell-cell interactions. *Cell Stem Cell* **3**, 289–300 (2008).
10. E. Kokovay *et al.*, Adult SVZ lineage cells home to and leave the vascular niche via differential responses to SDF1/CXCR4 signaling. *Cell Stem Cell* **7**, 163–173 (2010).
11. D. Coveney, J. Cool, T. Oliver, B. Capel, Four-dimensional analysis of vascularization during primary development of an organ, the gonad. *Proc. Natl. Acad. Sci. U.S.A.* **105**, 7212–7217 (2008).
12. J. Cool, T. J. DeFalco, B. Capel, Vascular-mesenchymal cross-talk through Vegf and Pdgf drives organ patterning. *Proc. Natl. Acad. Sci. U.S.A.* **108**, 167–172 (2011).
13. A. N. Combes *et al.*, Endothelial cell migration directs testis cord formation. *Dev. Biol.* **326**, 112–120 (2009).
14. D. L. Kumar, T. DeFalco, A perivascular niche for multipotent progenitors in the fetal testis. *Nat. Commun.* **9**, 4519 (2018).
15. T. Svingen, M. François, D. Wilhelm, P. Koopman, Three-dimensional imaging of Prox1-EGFP transgenic mouse gonads reveals divergent modes of lymphangiogenesis in the testis and ovary. *PLoS One* **7**, e52620 (2012).
16. M. Bullejos, J. Bowles, P. Koopman, Extensive vascularization of developing mouse ovaries revealed by caveolin-1 expression. *Dev. Dyn.* **225**, 95–99 (2002).
17. R. M. McFee *et al.*, Inhibition of vascular endothelial growth factor receptor signal transduction blocks follicle progression but does not necessarily disrupt vascular development in perinatal rat ovaries. *Biol. Reprod.* **81**, 966–977 (2009).
18. M. Wagner *et al.*, Single-cell analysis of human ovarian cortex identifies distinct cell populations but no oogonial stem cells. *Nat. Commun.* **11**, 1147 (2020).
19. R. D. Prasasya, K. E. Mayo, Notch signaling regulates differentiation and steroidogenesis in female mouse ovarian granulosa cells. *Endocrinology* **159**, 184–198 (2018).
20. B. Lloyd-Lewis, P. Mourikis, S. Fre, Notch signalling: Sensor and instructor of the microenvironment to coordinate cell fate and organ morphogenesis. *Curr. Opin. Cell Biol.* **61**, 16–23 (2019).
21. D. A. Vanorny, K. E. Mayo, The role of Notch signaling in the mammalian ovary. *Reproduction* **153**, R187–R204 (2017).
22. Y. M. Feng *et al.*, Notch pathway regulates female germ cell meiosis progression and early oogenesis events in fetal mouse. *Cell Cycle* **13**, 782–791 (2014).
23. C. Wiese *et al.*, Nestin expression–A property of multi-lineage progenitor cells? *Cell. Mol. Life Sci.* **61**, 2510–2522 (2004).
24. M. H. Jiang *et al.*, Characterization of Nestin-positive stem Leydig cells as a potential source for the treatment of testicular Leydig cell dysfunction. *Cell Res.* **24**, 1466–1485 (2014).
25. M. S. Davidoff *et al.*, Progenitor cells of the testosterone-producing Leydig cells revealed. *J. Cell Biol.* **167**, 935–944 (2004).
26. C. F. Liu, C. Liu, H. H. Yao, Building pathways for ovary organogenesis in the mouse embryo. *Curr. Top. Dev. Biol.* **90**, 263–290 (2010).
27. I. Stévant *et al.*, Dissecting cell lineage specification and sex fate determination in gonadal somatic cells using single-cell transcriptomics. *Cell Rep.* **26**, 3272–3283.e3 (2019).
28. Y. Ikeda, W. H. Shen, H. A. Ingraham, K. L. Parker, Developmental expression of mouse steroidogenic factor-1, an essential regulator of the steroid hydroxylases. *Mol. Endocrinol.* **8**, 654–662 (1994).
29. J. Pelletier *et al.*, Expression of the Wilms' tumor gene WT1 in the murine urogenital system. *Genes Dev.* **5**, 1345–1356 (1991).
30. G. Wu, Q. Wei, D. Yu, F. Shi, Neonatal genistein exposure disrupts ovarian and uterine development in the mouse by inhibiting cellular proliferation. *J. Reprod. Dev.* **65**, 7–17 (2019).
31. C. Zeltz *et al.*, α11β1 integrin is induced in a subset of cancer-associated fibroblasts in desmoplastic tumor stroma and mediates in vitro cell migration. *Cancers (Basel)* **11**, 765 (2019).
32. F. Kizuka *et al.*, Involvement of bone marrow-derived vascular progenitor cells in neovascularization during formation of the corpus luteum in mice. *Biol. Reprod.* **87**, 55 (2012).
33. V. P. Jovanovic *et al.*, Intraovarian regulation of gonadotropin-dependent folliculogenesis depends on notch receptor signaling pathways not involving Delta-like ligand 4 (Dll4). *Reprod. Biol. Endocrinol.* **11**, 43 (2013).
34. J. S. Richards, Y. A. Ren, N. Candelaria, J. E. Adams, A. Rajkovic, Ovarian follicular theca cell recruitment, differentiation, and impact on fertility: 2017 update. *Endocr. Rev.* **39**, 1–20 (2018).
35. D. A. Vanorny, R. D. Prasasya, A. J. Chalpe, S. M. Kilen, K. E. Mayo, Notch signaling regulates ovarian follicle formation and coordinates follicular growth. *Mol. Endocrinol.* **28**, 499–511 (2014).
36. S. Nowotschin, P. Xenopoulos, N. Schrode, A. K. Hadjantonakis, A bright single-cell resolution live imaging reporter of Notch signaling in the mouse. *BMC Dev. Biol.* **13**, 15 (2013).
37. Z. Liu *et al.*, The extracellular domain of Notch2 increases its cell-surface abundance and ligand responsiveness during kidney development. *Dev. Cell* **25**, 585–598 (2013).
38. A. Ivanova *et al.*, In vivo genetic ablation by Cre-mediated expression of diphtheria toxin fragment A. *Genesis* **43**, 129–135 (2005).
39. F. E. Duncan *et al.*, Age-associated dysregulation of protein metabolism in the mammalian oocyte. *Aging Cell* **16**, 1381–1393 (2017).
40. T. Suzuki *et al.*, Cyclic changes of vasculature and vascular phenotypes in normal human ovaries. *Hum. Reprod.* **13**, 953–959 (1998).
41. A. Bernal, L. Arranz, Nestin-expressing progenitor cells: Function, identity and therapeutic implications. *Cell. Mol. Life Sci.* **75**, 2177–2195 (2018).
42. N. Takahashi, M. T. Itoh, B. Ishizuka, Human chorionic gonadotropin induces nestin expression in endothelial cells of the ovary via vascular endothelial growth factor signaling. *Endocrinology* **149**, 253–260 (2008).
43. A. McLaren, Development of the mammalian gonad: The fate of the supporting cell lineage. *BioEssays* **13**, 151–156 (1991).
44. K. H. Albrecht, E. M. Eicher, Evidence that Sry is expressed in pre-Sertoli cells and Sertoli and granulosa cells have a common precursor. *Dev. Biol.* **240**, 92–107 (2001).
45. J. Karl, B. Capel, Sertoli cells of the mouse testis originate from the coelomic epithelium. *Dev. Biol.* **203**, 323–333 (1998).
46. L. Lei, A. C. Spradling, Mouse primordial germ cells produce cysts that partially fragment prior to meiosis. *Development* **140**, 2075–2081 (2013).
47. M. Uda *et al.*, Foxl2 disruption causes mouse ovarian failure by pervasive blockage of follicle development. *Hum. Mol. Genet.* **13**, 1171–1181 (2004).
48. A. Ng *et al.*, Lgr5 marks stem/progenitor cells in ovary and tubal epithelia. *Nat. Cell Biol.* **16**, 745–757 (2014).
49. D. J. Trombly, T. K. Woodruff, K. E. Mayo, Suppression of Notch signaling in the neonatal mouse ovary decreases primordial follicle formation. *Endocrinology* **150**, 1014–1024 (2009).
50. J. Xu, T. Gridley, Notch2 is required in somatic cells for breakdown of ovarian germ-cell nests and formation of primordial follicles. *BMC Biol.* **11**, 13 (2013).
51. K. J. Terauchi, Y. Shigeta, T. Iguchi, T. Sato, Role of Notch signaling in granulosa cell proliferation and polyovular follicle induction during folliculogenesis in mouse ovary. *Cell Tissue Res.* **365**, 197–208 (2016).
52. W. Zheng *et al.*, Two classes of ovarian primordial follicles exhibit distinct developmental dynamics and physiological functions. *Hum. Mol. Genet.* **23**, 920–928 (2014).
53. S. A. Cicero *et al.*, Cells previously identified as retinal stem cells are pigmented ciliary epithelial cells. *Proc. Natl. Acad. Sci. U.S.A.* **106**, 6685–6690 (2009).
54. Z. Liu, A. C. Obenauf, M. R. Speicher, R. Kopan, Rapid identification of homologous recombinants and determination of gene copy number with reference/query pyrosequencing (RQPS). *Genome Res.* **19**, 2081–2089 (2009).
55. K. Tanigaki *et al.*, Notch-RBP-J signaling is involved in cell fate determination of marginal zone B cells. *Nat. Immunol.* **3**, 443–450 (2002).
56. S. Bolte, F. P. Cordelières, A guided tour into subcellular colocalization analysis in light microscopy. *J. Microsc.* **224**, 213–232 (2006).
57. C. Zeng *et al.*, Evaluation of 5-ethynyl-2′-deoxyuridine staining as a sensitive and reliable method for studying cell proliferation in the adult nervous system. *Brain Res.* **1319**, 21–32 (2010).
58. S. K. Bristol-Gould *et al.*, Postnatal regulation of germ cells by activin: The establishment of the initial follicle pool. *Dev. Biol.* **298**, 132–148 (2006).
59. T. Sato *et al.*, In vitro production of functional sperm in cultured neonatal mouse testes. *Nature* **471**, 504–507 (2011).
60. T. DeFalco, I. Bhattacharya, A. V. Williams, D. M. Sams, B. Capel, Yolk-sac-derived macrophages regulate fetal testis vascularization and morphogenesis. *Proc. Natl. Acad. Sci. U.S.A.* **111**, E2384–E2393 (2014).